Applied Catalysis B: Environmental 88 (2009) 542–549

Contents lists available at ScienceDirect

Applied Catalysis B: Environmental

journal homepage: www.elsevier.com/locate/apcatb

Enhancement of oxygen storage capacity by reductive treatment of Al_2O_3 and CeO_2–ZrO_2 solid solution nanocomposite

Akira Morikawa [a,*], Koichi Kikuta [b], Akihiko Suda [a], Hirofumi Shinjo [a]

[a] Catalyst Lab., Toyota Central R&D Labs., Inc., 41-1 Yokomichi, Nagakute, Nagakute-Cho, Aichi-Gun, Aichi 480-1192, Japan
[b] Department of Crystalline Materials Science, Graduate School of Engineering, Nagoya University, Furo-Cho, Chikusa-Ku, Nagoya, Aichi 464-8603, Japan

ARTICLE INFO

Article history:
Received 10 June 2008
Received in revised form 23 September 2008
Accepted 15 October 2008
Available online 6 November 2008

Keywords:
Al_2O_3
CeO_2
ZrO_2
Oxygen storage capacity
Reduction

ABSTRACT

Oxygen storage capacity (OSC) of CeO_2–ZrO_2 solid solution, $Ce_xZr_{(1-x)}O_4$, is one of the most contributing factors to control the performance of an automotive catalyst. To improve the OSC, heat treatments were employed on a nanoscaled composite of Al_2O_3 and $CeZrO_4$ (ACZ). Reductive treatments from 700 to 1000 °C significantly improved the complete oxygen storage capacity (OSC-c) of ACZ. In particular, the OSC-c measured at 300 °C reached the theoretical maximum with a sufficient specific surface area (SSA) (35 m^2/g) after reductive treatment at 1000 °C. The introduced Al_2O_3 facilitated the regular rearrangement of Ce and Zr ions in $CeZrO_4$ as well as helped in maintaining the sufficient SSA. Reductive treatments also enhanced the oxygen release rate (OSC-r); however, the OSC-r variation against the evaluation temperature and the reduction temperature differed from that of OSC-c. OSC-r measured below 200 °C reached its maximum against the reduction temperature at 800 °C, while those evaluated at 300 °C increased with the reduction temperature in the same manner as OSC-c.

1. Introduction

Among the automotive three-way catalysts, CeO_2–ZrO_2 solid solution ($Ce_xZr_{(1-x)}O_4$) is an indispensable component that acts as an oxygen storage material [1]. Its oxygen storage capacity (OSC) buffers the lean-rich swings to achieve a stoichiometric atmosphere with an air/fuel ratio of about 14.6. Thus, the exhaust gases of hydrocarbons (HC), CO, and NO_x are efficiently converted [1,2]. Furthermore, the catalyst with much larger OSC indicates the higher catalytic performance [3], in other words, the improvement of OSC performance achieves the advanced level of catalysts. Initially, OSC materials were mainly employed as co-catalysts; however, they have been recently employed as supports to load catalytic metals such as Pt, Pd, and Rh. Therefore, OSC materials are those that offer both superior heat resistance and higher OSC performance [4]. Many studies [3–10] have focused on these goals, among which the most promising is a nanoscaled composite of Al_2O_3 and $CeZrO_4$ (CZ) called ACZ [3]. This material is proposed as an OSC material that offers better heat resistance. The introduced Al_2O_3 into ACZ behaves as a diffusion barrier to minimize the contacting of CZ, thereby suppressing CZ particle growth (Fig. 1). This improves heat resistance and OSC performance, particularly the oxygen release rate [11].

However, strict restrictions on automotive emissions (EURO6, LEVII, and J-SULEV) demand higher catalytic activity at lower temperatures, especially for HC [12]. Because activated oxygen released from OSC materials could be effective in eliminating HC at lower temperatures, the enhancement of OSC performance at lower temperatures is considered a key technology.

Although the availability of reductive treatments on OSC materials at high temperatures has been reported [13–17], materials reduced at high temperatures have no practical application because of their extremely low specific surface area (SSA).

In this study, ACZ with superior heat resistance as well as improved OSC performance is treated at high temperatures under various atmospheric conditions to advance OSC performance, while maintaining a sufficient SSA. This research could provide some principles for the development of next-generation OSC materials.

2. Experimental

2.1. Preparation of catalysts

ACZ was prepared as mentioned previously [11]. The molecular ratio of composition of Al_2O_3, CeO_2, and ZrO_2 was 1:1:1. 50 g of ACZ was placed in a quartz tube, and then treated at 700 °C for 5 h under the atmosphere of H_2 (5%)/N_2 with a flow rate of 1000 cm^3/min.

* Corresponding author. Tel.: +81 561 71 7492; fax: +81 561 63 6150.
E-mail address: a-morikawa@mosk.tytlabs.co.jp (A. Morikawa).

0926-3373/$ – see front matter © 2008 Elsevier B.V. All rights reserved.
doi:10.1016/j.apcatb.2008.10.019

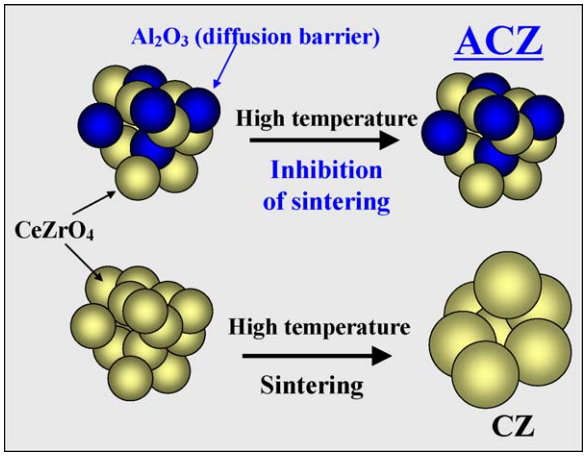

Fig. 1. Schematic diagram of the Al_2O_3 diffusion barrier concept to inhibit sintering of $CeZrO_4$.

For eluding the influence of various heat treatments on Pt dispersion, Pt loading process was performed after each heat treatment of ACZ. The reduced ACZ was added into the appropriate amount of aqueous solution of $Pt(NO_2)_2(NH_3)_2$ (Tanaka Precious Metals). After stirring for 3 h, the resulting solution was heated by a hot stirrer and the solvent was evaporated for loading all amount of Pt uniformly. The resulting powder was dried at 120 °C in air for 6 h and then calcined at 300 °C in air. The amount of Pt loaded on the reduced ACZ was 2 wt%. The obtained catalyst powder was compressed with a cold isostatic press and broken into catalyst pellets with diameters between 0.5 and 1 mm. Hereafter, this pellet catalyst is referred to as ACZ-H2-700. For a comparative study, catalysts treated between 800 and 1000 °C, or under a nitrogen atmosphere or air, as shown in Table 1. Moreover, to clarify the effect of the amount of additional Al_2O_3 in ACZ, CZ-H2-1000, A2CZ-H2-1000 catalysts were prepared in the same manner as the reduced ACZ catalysts. The molecular ratio of composition of Al_2O_3, CeO_2, and ZrO_2 in A2CZ was 2:1:1. The Al_2O_3 contents of CZ-H2-1000, ACZ-H2-1000, and A2CZ-H2-1000 catalysts were 0, 33.3, and 50 mol%. Each support was reduced at 1000 °C, prior to loading Pt.

2.2. Evaluation of catalysts

The SSA of each catalyst was measured by Brunauer–Emmett–Teller (BET) one-point method, using an automatic surface area analyzer (MICRO SORP-4232II, Micro Data) [11]. X-ray diffraction (XRD) patterns of catalysts at diffraction angles (2θ) from 10 to 80° were analyzed by an X-ray apparatus (RINT-TTR, RIGAKU) with Cu Kα radiation (λ = 1.5418 Å, 50 kV, 300 mA). Crystal phases of $CeZrO_4$ were assigned, and the diameters of crystallite were calculated from full width at half maximum of (1 1 1) lattice planes, according to Scherrer's equation [18]. Pt particle sizes in the catalysts were evaluated using a CO pulse adsorption apparatus (type-R6015, Okurariken). After pretreatment under conditions recommended by the Catalysis Society of Japan [19,20], catalysts were cooled in a dry ice/ethanol bath, and measurements were carried out at about −70 °C [11]. In general, OSC was classified into two types: OSC complete (OSC-c), which is the quantity of all releasable oxygen in the catalysts at a predetermined temperature, and the OSC rate (OSC-r), which is the releasable rate of oxygen [11]. OSC-c was measured according to the method proposed by Suda et al. [8–10]. The 2 wt% Pt-loaded catalyst was placed in a thermogravimetric analyzer (TGA-50, Okurariken) and pretreated at 500 °C for 15 min under an O_2 (20%)/N_2 (balance) atmosphere. After pretreatment, it was cooled to 300 °C in the same oxidative atmosphere. When the temperature reached the predetermined temperature, the atmosphere was switched from O_2 (20%)/N_2 to H_2 (20%)/N_2 until the weight decrease of the catalyst was no longer detected. Subsequently, the atmosphere was changed back to O_2 (20%)/N_2, and the atmosphere and temperature were maintained until the weight increase in the catalyst was no longer detected. These steps were repeated until the weight reduction under H_2 (20%)/N_2 and weight increase under O_2 (20%)/N_2 became almost equal. Subsequently, additional two cycles were repeated, followed by calculation of the average of each weight reduction and increase. The saturated OSC, OSC-c, was denoted as the amount of O_2 adsorption/desorption per mole of CeO_2 included in the catalyst (O_2-mol · CeO_2-mol^{-1}) [11].

The oxygen release rate, OSC-r, was derived by evaluating the amount of CO_2 formation under an alternative atmosphere, where CO (2%)/N_2 and O_2 (1%)/N_2 were introduced into a catalyst every 3 min, using a fixed-bed flow-type reaction apparatus (CATA5000-4, Best SOKKI) [11,21]. 1 g of a catalyst was filled in a quartz reaction tube with a diameter of 15 mm, and each reaction gas was introduced into the reaction tube with the flow rate of 5 L/min at the determined temperature. In this measurement, the gradient of the tangential line to the CO_2 production curve was the amount of oxygen released per second. CO and CO_2 were analyzed by a non-dispersive infrared (ND-IR) type analyzer and O_2 was quantified with a magnetic oxygen analyzer [11].

To evaluate the interaction between Pt and Ce, temperature programmed reduction (TPR) analysis with hydrogen was performed in a flow-type reactor (TP5000, Okurariken) coupled to a quadrupole mass spectrometer (RG-102P, ULVAC). 0.15 g of catalyst was pretreated at 300 °C for 10 min in O_2 (10%)/Ar and for 10 min in pure Ar prior to reduction. After cooling down to room temperature, H_2 (5%)/Ar flowed through the catalyst at 60 cm^3/min, raising the temperature at a heating rate of 20 °C/min up to 800 °C.

Table 1
Prepared catalysts.

Catalysts[a]	Atmosphere of heat-treatment[b]	Temperature (°C)
ACZ	–	–
ACZ-air-1000	Air	1000
ACZ-N2-1000	N_2	1000
ACZ-H2-700	H_2 (5%)/N_2	700
ACZ-H2-800	H_2 (5%)/N_2	800
ACZ-H2-900	H_2 (5%)/N_2	900
ACZ-H2-1000	H_2 (5%)/N_2	1000
CZ[c]-H2-1000	H_2 (5%)/N_2	1000
A2CZ[d]-H2-1000	H_2 (5%)/N_2	1000

[a] 2 wt% of Pt were loaded on all catalysts.
[b] Flow rate for all treatment gases was 1000 cm^3/min.
[c] CZ was composed only of the $CeZrO_4$ oxide.
[d] A2CZ had a twofold amount of Al_2O_3 to ACZ in molar ratio.

3. Results and discussion

3.1. Effect of treatment atmospheres

As shown in Table 2, the SSA of catalysts respectively treated in air, N_2, or H_2 (5%)/N_2 decreased down to about 40 m^2/g, and the SSA decrease ratios of these catalysts were almost the same, and there seemed no influence from the pretreatment atmosphere. On the other hand, $CeZrO_4$ crystallite sizes, obtained by XRD analysis, were 9.7, 11.5, and 14.8 nm for ACZ-air-1000, ACZ-N2-1000, and ACZ-H2-1000, respectively, as shown in Table 2. This indicates that the crystallite in the catalyst sinters more significantly after treatment in an atmosphere containing less oxygen and more reductant. The crystallite growth of $CeZrO_4$ in ACZ-H2-1000 can be

Table 2
Characterization of SSA, $CeZrO_4$ crystallite sizes, and Pt particle sizes for catalysts treated in different conditions.

Catalysts	SSA[a] ($m^2\ g^{-1}$)	$CeZrO_4$ crystallite size[b] (nm)	$I_{(15/29)}$[c]	Pt particle size[d] (nm)
ACZ	103	6.4	–	0.8
ACZ-air-1000	37	9.7	–	1.1
ACZ-N2-1000	36	11.5	–	1.1
ACZ-H2-700	97	8.4	–	0.9
ACZ-H2-800	76	8.7	–	1
ACZ-H2-900	45	10.2	–	1.1
ACZ-H2-1000	32	14.8	0.033	1.4
ACZ-H2-1000a[e]	31	15.0	0.033	1.4
CZ-H2-1000	1	21.4	0.008	2.6
A2CZ-H2-1000	55	11.6	0.033	1.2

[a] N_2 or N_2 (30%)/He (balance) flow at the rate of 25 cm^3/min per quartz reaction pipe. A "U" type quartz pipe was used.
[b] Cu Kα-2 was eliminated with Jade ver. 7 software.
[c] $I_{(15/29)}$ indicates the relative intensity of the diffraction peak of $2\theta = 15^\circ$ to $2\theta = 29^\circ$.
[d] Pt particle sizes were analyzed using the low-temperature CO pulse adsorption method [11].
[e] This catalyst indicates ACZ-H2-1000 after OSC-c measurement at 500 °C.

achieved by an increase in the diffusion rate of Ce and Zr ions in the crystallite. In other words, high-temperature reduction could facilitate the bulk diffusion of Ce and Zr ions due to the increased number of Ce^{3+} ions and oxygen defects in the $CeZrO_4$ crystallites [14–17]. Each catalyst XRD pattern shown in Fig. 2 indicates one crystal phase of the $CeZrO_4$ solid solution, and this phase was maintained after the high-temperature treatment. Moreover, this crystal phase in ACZ, ACZ-air-1000, and ACZ-N2-1000 was assigned to the fluorite phase or t″-phase, which has an arrangement of Ce and Zr cations identical to a fluorite structure, and lower symmetry of oxygen ions [22–24]. On the other hand, the crystal phase of $CeZrO_4$ in ACZ-H2-1000 was identified as κ-phase, which has regularly arranged Ce and Zr ions in the $CeZrO_4$ lattice [22–25]. This means that Ce and Zr cations in the crystallite rearrange during the reductive treatment at 1000 °C [13]. In addition, ACZ-H2-1000 only showed weak diffraction peaks around 24° and 41° of 2θ, assigned to $CeAlO_3$ [26,27]. This implies that Al_2O_3 interacts with $CeZrO_4$. However, the XRD pattern of (e) in Fig. 2 (ACZ-H2-1000a), which was taken after OSC-c measurement at 500 °C in alternative atmosphere between H_2/N_2 and O_2/N_2 did not change from that of initial ACZ-H2-1000 (pattern (d) in Fig. 2). These diffraction peaks assigned to $CeZrO_4$ in ACZ-H2-1000 before and after OSC-c measurement did not shift against corresponding those in other heated catalysts. Furthermore, OSC-c of ACZ-H2-1000 above 300 °C indicated a theoretical maximum as discussed below. These results suggest the following two notions: (i) almost all the fluorite phase or t″-phase transformed to the κ-phase in ACZ-H2-1000, (ii) extremely small amounts of $CeAlO_3$ could be formed and this phase hardly contributes OSC-c.

OSC-c measured by thermogravimetric analysis at 100, 300, and 500 °C is shown in Fig. 3. The OSC-c of both ACZ-air-1000 and ACZ-N2-1000 measured at three temperature stages was almost identical to that of ACZ without heat treatments. These results indicate that treatment with air or N_2 does not affect the OSC-c of ACZ. ACZ-H2-1000, however, showed an OSC-c about 2.5 times larger than that of ACZ measured at 100 °C. Furthermore, this catalyst exhibited the theoretical maximum of OSC-c when analyzed at 300 °C. Thus, according to Eq. (1), above 300 °C, all Ce^{4+} ions are completely reduced to Ce^{3+} (Ce-reductive efficiency is 100%):

$$Ce(VI)O_2 \Leftrightarrow \tfrac{1}{2}Ce(III)_2O_3 + \tfrac{1}{4}O_2 \quad (1)$$

Previous studies have reported improvement in OSC through reductive treatments [14–17] or by chemical filling of OSC

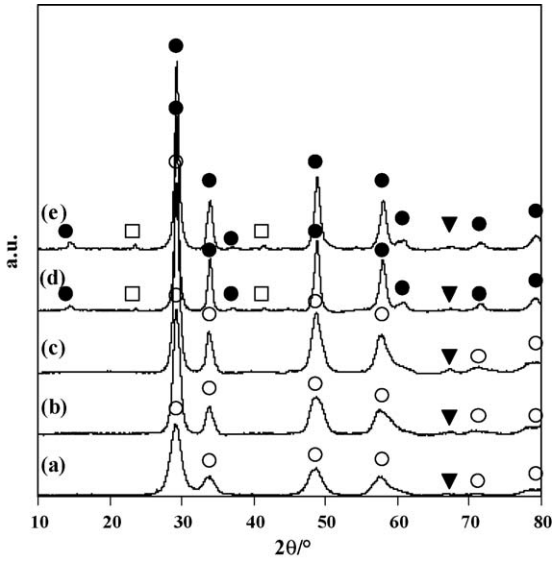

Fig. 2. XRD patterns of ACZ catalysts: (a) as obtained (fresh), (b) calcined in air at 1000 °C, (c) calcined in N_2 at 1000 °C, and (d) reduced in H_2 (5%)/N_2 at 1000 °C. The pattern (e) indicates that of (d) after OSC-c measurement at 500 °C. All catalysts were treated prior to Pt loading. (●) κ-Phase of $CeZrO_4$; (○) fluorite or t″-phase of $CeZrO_4$; (▼) γ-Al_2O_3; (□) $CeAlO_3$.

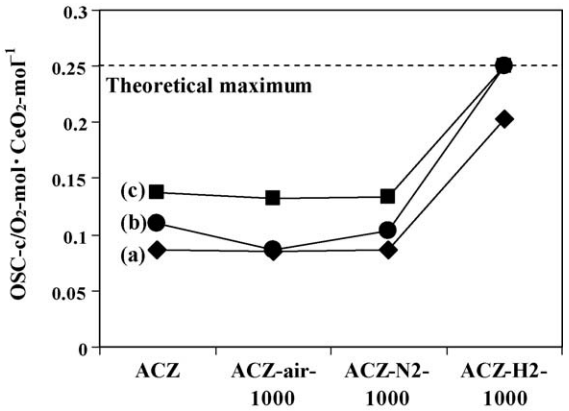

Fig. 3. OSC-c of ACZ catalysts treated in various atmospheres prior to Pt loading. ACZ: fresh; ACZ-air-1000: calcined in air at 1000 °C for 5 h; ACZ-N2-1000: calcined in N_2 at 1000 °C for 5 h; ACZ-H2-1000: reduced in H_2 (5%)/N_2 at 1000 °C for 5 h. (a) Measured at 100 °C; (b) measured at 300 °C; (c) measured at 500 °C. The dotted-line shows the theoretical maximum, which corresponds to the state of that $Ce_2Zr_2O_7$ in a reductive atmosphere and $Ce_2Zr_2O_8$ in an oxidation condition.

materials produced in a reductive atmosphere [28,29]. Moreover, a Pt/CeO_2–ZrO_2 catalyst, reduced at 1200 °C prior to Pt loading, with 88.6% of the Ce reductive efficiency at 500 °C was also reported, although this had a significantly low SSA of 1 m^2/g [23]. Therefore, ACZ-H2-1000 is the first example of an OSC material with a mole ratio of Ce/Zr around 1/1, which indicates almost 100% Ce reductive efficiency at a lower temperature of 300 °C, as well as keeping the practical SSA (35 m^2/g). ACZ-H2-1000 showed Pt particle sizes twice that of fresh ACZ, as shown in Table 2. Although Pt particles are generally considered as active sites for oxygen releasing or absorption, ACZ-H2-1000, which had the highest OSC-c, also had the largest Pt particle size. This implies that OSC-c depends on the properties of oxygen in the $CeZrO_4$ lattice, rather than Pt particle size [11,30].

The OSC-r for each catalyst is shown in Fig. 4. The measurements were carried out in the region between 100 and 300 °C, where the conversion of reaction gas was less than 30% to eliminate the effect of the reactant supply or diffusion rate on the reaction [31].

Each catalyst showed an almost identical OSC-r value at 100 °C, and ACZ-H2-1000 and ACZ had an OSC-r twice as large as other catalysts at 200 °C. On the other hand, at 300 °C, only the OSC-r of ACZ-H2-1000 was twice as that of others. The Pt particle size was double that of ACZ in ACZ-H2-1000, and that of ACZ-air-1000 or ACZ-N2-1000 was 1.4 times that of ACZ. These results suggest that the rate determination step of O_2 release reaction with CO varies with the measurement temperature. At 100 °C, little surface oxygen could react with CO because the catalyst is not sufficiently activated at this temperature. Since oxygen on or near the surface could react with CO at 200 °C, and ACZ has the highest SSA and smallest Pt particle size among these four catalysts, thus the OSC-r of ACZ increased much larger than the rest of catalyst when temperature was raised from 100 to 200 °C. In contrast, ACZ-H2-1000, with the lowest SSA and largest Pt particle size, showed an almost identical OSC-r to ACZ at 200 °C, due to the production of highly mobile oxygen on or near the surface of the κ-phase [32]. The OSC-r of ACZ-air-1000 or ACZ-N2-1000 at 200 °C was almost the same as that at 100 °C, because they have no κ-phase. At 300 °C, since oxygen in the $CeZrO_4$ lattice could react with supplied CO, ACZ-H2-1000 with a large amount of highly mobile oxygen in the lattice showed a remarkably larger OSC-r than others; the OSC-r of ACZ-H2-1000 is three times larger than that at 200 °C. On the contrary, the increase in the OSC-r for ACZ from 200 to 300 °C was smaller than that for ACZ-H2-1000. This implies that oxygen on or near the surface could control the OSC-r of ACZ. Note that the OSC-r of ACZ-air-1000 or ACZ-N2-1000 increased more than that of ACZ as the measurement temperature increased from 200 to 300 °C. As stated above, although these two catalysts had almost one-third of SSA and much larger Pt particles, compared with ACZ, without formation of the κ-phase, the OSC-r gradually increased with the measurement temperature. These results suggest that the heat treatment in an atmosphere of N_2 or air changed the environment around the lattice oxygen. Alternatively, it is possible that CO adsorbed on ACZ-air-1000 or ACZ-N2-1000 at 200 °C does not spill over so far from Pt. These catalysts could show a smaller OSC-r than ACZ because of their lower Pt dispersion, while they could exhibit a larger OSC-r than ACZ owing to the movement of CO further from Pt in spite of the lower dispersion at 300 °C [30,32].

In H_2-TPR analysis, ACZ catalyst showed one peak around at 140 °C with a shoulder peak at around 180 °C, as shown in Fig. 5. Since Damyanova and Bueno reports that Pt interacts preferentially with the surface of CeO_2 even in the presence of a much larger surface area of Al_2O_3 [33], the oxidative state of Pt on ACZ is also mainly affected by not Al_2O_3 but the $CeZrO_4$ crystallite in ACZ. In addition, the reduction peak of $CeZrO_4$ loaded with Pt from 130 to 180 °C is assigned to the reduction of Pt oxide and to the reduction of $CeZrO_4$ by the reduced Pt as reported in previous studies [4,34–37]. Therefore, the corresponding peak of ACZ-H2-1000 catalyst shifted to higher, suggesting that the spill over of hydrogen becomes more difficult owing to enhancement of Pt–O–Ce interaction [38]. On the other hand, both ACZ-air-1000 and ACZ-N2-1000 indicated two peaks, the relatively sharp one at around 90 °C and the broad one at around 180 °C. The former is identified as the reduction of PtO or PtO_2 [36,39], and the latter is similarly identified as that of Pt and $CeZrO_4$. In addition, the relative intensity of the broad peak to the sharp peak of ACZ-N2-1000 catalyst was stronger than that of ACZ-air-1000. These results imply that the relative intensity of the peak at around 180 °C becomes stronger with decreasing the oxygen partial pressure during heat treatment of ACZ at 1000 °C prior to Pt loading, in other word, hydrogen spill over becomes difficult by decreasing the oxygen partial pressure during a preheat treatment. This could be attributed to the intensifying of Pt–O–Ce interaction. Although the

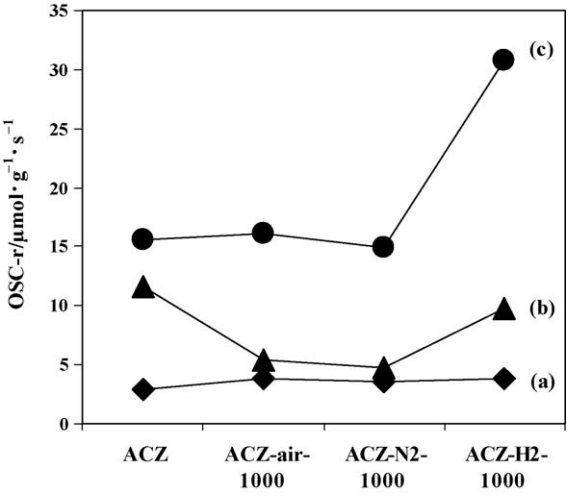

Fig. 4. OSC-r of ACZ catalysts measured using a fixed-bed flow-type reactor with alternative CO/N_2 and O_2/N_2 at (a) 100 °C, (b) 200 °C, and (c) 300 °C. ACZ: fresh (not treated); ACZ-air-1000: calcined in air at 1000 °C for 5 h; ACZ-N2-1000: calcined in N_2 at 1000 °C for 5 h; ACZ-H2-1000: reduced in H_2 (5%)/N_2 at 1000 °C for 5 h. All catalysts were preheated prior to Pt loading.

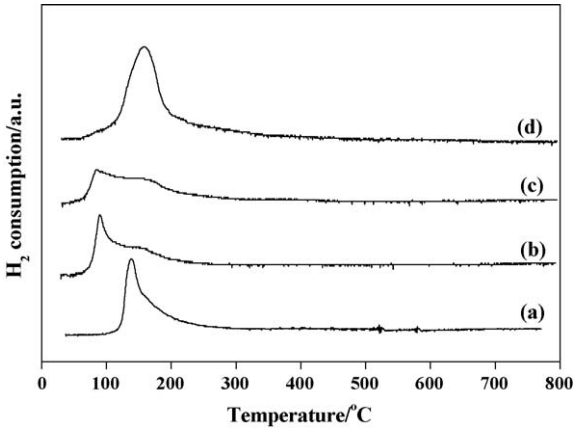

Fig. 5. H_2-TPR profiles of catalysts treated in various atmospheres. (a) ACZ: fresh (not treated); (b) ACZ-air-1000: calcined in air at 1000 °C for 5 h; (c) ACZ-N2-1000: calcined in N_2 at 1000 °C for 5 h; (d) ACZ-H2-1000: reduced in H_2 (5%)/N_2 at 1000 °C for 5 h. All catalysts were preheated prior to Pt loading.

reason for the interaction by atmosphere for preheat treatment is not obvious, it is likely that the concentration of Ce ions on the surface of the $CeZrO_4$ crystallite may affect the interaction between Pt and $CeZrO_4$ [40,41]. This behavior is corresponding to that of OSC-r measured at 200 °C. Namely, ACZ or ACZ-H2-1000 catalyst with intensifying peak at around 180 °C show the larger OSC-r than that of ACZ-air-1000 or ACZ-N2-1000 catalyst, which indicate significantly weaker peaks at same region.

These results suggest that both OSC-c and OSC-r can be improved by the heat treatment in reductive conditions.

Although the influence from oxygen diffusion should also be counted to their OSC rates, this point will be further discussed in Section 3.3 by considering the other physical parameters.

3.2. Effect of introducing an Al_2O_3 diffusion barrier during reductive treatments

As shown in Table 2, the SSA of CZ only composed of $CeZrO_4$ degraded to 1 m^2/g upon the reductive treatment at 1000 °C. This is in contrast to ACZ, which maintains an SSA of 35 m^2/g, as discussed in Section 3.1. Moreover, A2CZ maintained an SSA of 55 m^2/g. The growth of $CeZrO_4$ crystallite in ACZ and A2CZ was inhibited more than that in CZ, as shown in Table 2—CZ and ACZ had almost identical crystallite sizes in their initial condition (see Ref. [11]). This indicates that an Al_2O_3 diffusion barrier can suppress the crystallite growth of $CeZrO_4$ and restrict the degradation of the SSA with increasing the amount of added Al_2O_3 during the reductive treatment at 1000 °C. Fig. 6 shows XRD patterns of theses three catalysts. Although ACZ-H2-1000 and A2CZ-H2-1000 exhibit the characteristic XRD patterns for the κ-phase, as mentioned earlier, CZ-H2-1000 has only characteristic diffraction lines around 15° and 38° assigned to the κ-phase, which are comparatively weaker than those of others. Furthermore, CZ-H2-1000 showed a lower $I_{(15/29)}$ than the reduced ACZ catalysts did, as shown in Table 2. $I_{(15/29)}$ is defined as the relative intensity of the diffraction peak of $2\theta = 15°$ to $2\theta = 29°$. As the former peak is characteristic one of the κ-phase and the later peak of the κ-phase overlaps with the strongest one of the fluorite phase or t″-phase, the lower $I_{(15/29)}$ indicates the smaller amount of the κ-phase. Therefore, only a part of $CeZrO_4$, assigned to fluorite or t″-phase in CZ, could transform into the κ-phase. Moreover, CZ-H2-1000 shows a shoulder peak at around 2θ of 50°, which cannot be observed in other catalysts. This shoulder could indicate the production of the Zr-rich phase of $CeZrO_4$, also suggesting that an Al_2O_3 diffusion barrier stabilizes the $CeZrO_4$ crystallite.

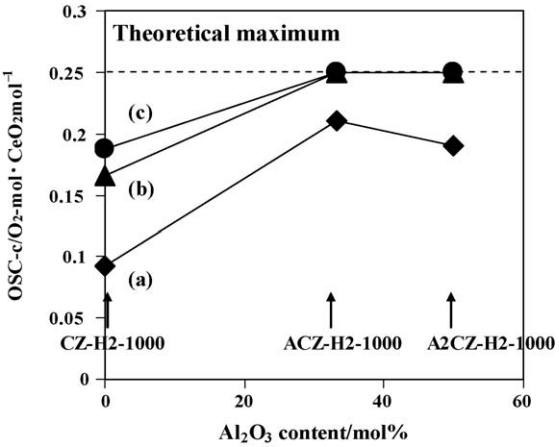

Fig. 7. OSC-c of catalysts as a function of Al_2O_3 molar ratio in ACZ. The measurement was performed using a thermogravimetric analyzer at (a) 100 °C, (b) 300 °C, and (c) 500 °C. Each catalyst was reduced in H_2 (5%)/N_2 at 1000 °C for 5 h prior to Pt loading. The dotted-line shows the theoretical maximum, which corresponds to the state of that $Ce_2Zr_2O_7$ in a reductive atmosphere and $Ce_2Zr_2O_8$ in an oxidation condition.

On the other hand, A2CZ-H2-1000 showed the same $I_{(15/29)}$ as ACZ-H2-1000. This fact suggests that the increase of Al_2O_3 content does not affect the feasibility of the formation of the κ-phase. It also seems that ACZ-H2-1000 has already included enough amount of Al_2O_3 as a diffusion barrier.

After the reductive treatment, CZ-H2-1000 showed improved OSC-c from 100 to 500 °C, compared with CZ (see Ref. [11]). However, CZ-H2-1000 underperformed ACZ-H2-1000 and A2CZ-H2-1000 on OSC-c at each measurement temperature, as shown in Fig. 7. Furthermore, the OSC-c of CZ-H2-1000 at 500 °C only showed about 80% of the theoretical maximum of 0.25, although ACZ-H2-1000 and A2CZ-H2-1000 reached the value of 0.25 already at 300 °C. These results also suggest that the κ-phase $CeZrO_4$ in CZ-H2-1000 could be formed partially.

The OSC-r of these three catalysts indicated a maximum value against the Al_2O_3 mol ratio of 33.3% above 200 °C. ACZ-H2-1000 (Al_2O_3 content was 33.3 mol%) outperformed other catalysts above 200 °C measurement temperature, as shown in Fig. 8. Since Pt sizes of ACZ-H2-1000 and A2CZ-H2-1000 (Al_2O_3 content was 50 mol%)

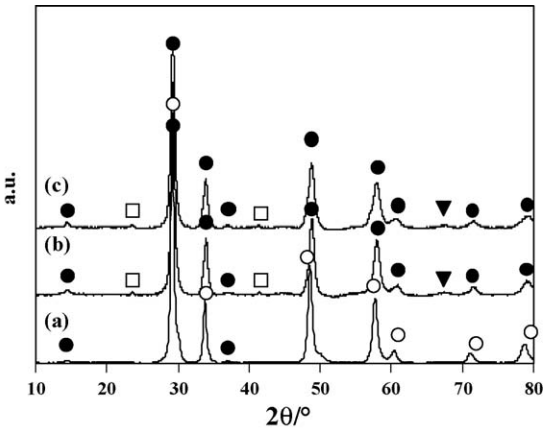

Fig. 6. XRD patterns of catalysts reduced prior to Pt loading. (a) CZ-H2-1000: reduced in H_2 (5%)/N_2 at 1000 °C; (b) ACZ-H2-1000: reduced in H_2 (5%)/N_2 at 1000 °C; (c) A2CZ-H2-1000: reduced in H_2 (5%)/N_2 at 1000 °C. (●) κ-Phase of $CeZrO_4$; (○) fluorite or t″-phase of $CeZrO_4$; (▼) γ-Al_2O_3; (□) $CeAlO_3$.

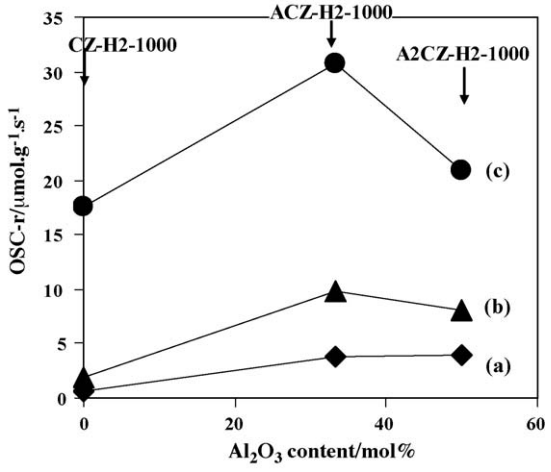

Fig. 8. OSC-r of catalysts as a function of Al_2O_3 molar ratio in ACZ. The measurement was performed using a fixed-bed flow-type reactor with alternative CO/N_2 and O_2/N_2 at (a) 100 °C, (b) 200 °C, and (c) 300 °C. Each catalyst was reduced in H_2 (5%)/N_2 at 1000 °C for 5 h prior to Pt loading.

were almost same shown in Table 2, the appropriate amount of introduced of Al_2O_3 diffusion barrier increases the activity of Pt–$CeZrO_4$ interface as active sites and improves its OSC-r (ACZ-H2-1000). On the other hand, too much amount of additional Al_2O_3 decreases interfaces between Pt and $CeZrO_4$ crystallite for a certain amount of Pt, and consequently the OSC-r of A2CZ-H2-1000 underperforms that of ACZ-H2-1000.

These results also indicate that, with Al_2O_3 introduction as a diffusion barrier, the Ce and Zr ions are more easily re-arranged by the reductive treatment and highly mobile oxygen are more apt to be produced in the $CeZrO_4$ lattice of ACZ or A2CZ than in that of CZ. This easier rearrangement of Ce and Zr ions could be attributed to better diffusion of the two ions in $CeZrO_4$ crystallite when Al_2O_3, introduced as a diffusion barrier, suppresses the crystallite growth. The excess introduction of Al_2O_3, however, decreases OSC-r because of decreasing the number of active sites because of a certain amount of Pt lost interaction with $CeZrO_4$ crystallite as discussed earlier.

3.3. Effect of reductive temperature

The SSA of ACZ gradually decreased with increased reductive temperature, particularly above 900 °C, as shown in Table 2. Accompanying this degradation, the $CeZrO_4$ crystallite sintered, which grew twofold at 1000 °C, compared with treatment at 700 °C, as shown in Table 2. XRD patterns of ACZ heated in a reductive atmosphere below 800 °C exhibit the diffraction line assigned to fluorite or t″-phase $CeZrO_4$, as shown in Fig. 9b and c. On the other hand, ACZ-H2-900 (Fig. 9d) shows a significantly broad peak around $2\theta = 14.5^\circ$ in addition to the line identified as fluorite or the t″-phase of $CeZrO_4$. This could be assigned to one of the characteristic peaks in the κ-phase [22–25], suggesting that some Ce and Zr ions in the $CeZrO_4$ lattice had already begun to rearrange regularly. Hence, the significant crystallite growth of $CeZrO_4$ above 900 °C is thought to be accelerated by the phase transition because of the formation of the definite κ-phase of $Ce_2Zr_2O_8$ in ACZ-H2-1000. No other diffraction lines were detected in any of the reduced catalysts, except for a broad peak at around $2\theta = 68^\circ$ assigned to γ-Al_2O_3 below 900 °C. The formation of $CeAlO_3$ by the reaction of Al_2O_3 with CeO_2 was reported in a previous study [27], according to which $CeAlO_3$ was prepared by reductive treatments above 900 °C. In our experiment, the diffraction line identified as $CeAlO_3$ was observed only after reduction at 1000 °C, as shown in Fig. 9e. Moreover, the amount of detected $CeAlO_3$ in ACZ-H2-1000 was small, indicating that the formation reaction of $CeAlO_3$ was successfully suppressed, and the nanocomposite structure of Al_2O_3 and $Ce_2Zr_2O_8$ was maintained. The suppression of the formation reaction of $CeAlO_3$ might be caused by the higher stability of the combination of pyrochlore-phase $Ce_2Zr_2O_7$ [40,42] and Al_2O_3 in a reduction atmosphere than that of $CeAlO_3$ and ZrO_2 or others. In the reduction atmosphere, the κ-phase of $Ce_2Zr_2O_8$ transforms into pyrochlore-phase $Ce_2Zr_2O_7$.

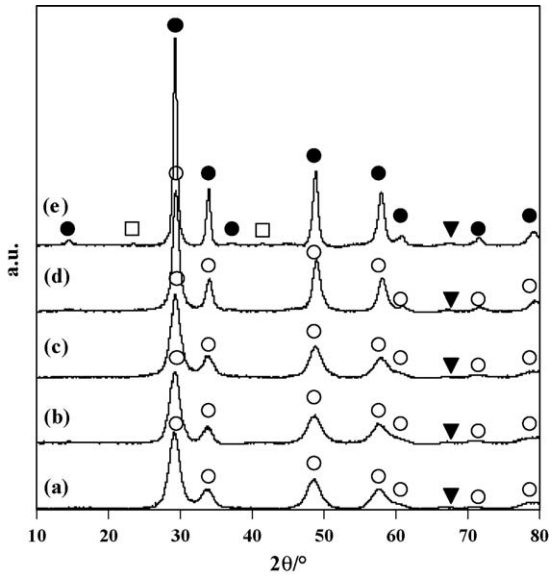

Fig. 9. XRD patterns of ACZ catalysts reduced in H_2 (5%)/N_2 (a) fresh (not reduced), (b) at 700 °C, (c) at 800 °C, (d) at 900 °C, and (e) at 1000 °C, for 5 h. All catalysts were treated prior to Pt loading. (●) κ-Phase of $CeZrO_4$; (○) fluorite or t″-phase of $CeZrO_4$; (▼) γ-Al_2O_3; (□) $CeAlO_3$.

OSC-c of ACZ catalysts was enhanced by the reduction and increased with the reduction temperature at each measurement temperature, as shown in Fig. 10. ACZ-H2-900 showed the OSC-c reaching about 90% of its theoretical maximum at 300 °C. The results of XRD suggest that this could contribute to the formation of more Ce and Zr ions regularly rearranged in ACZ-H2-900, compared with those in ACZ, reduced at lower temperatures. Further, Pt particle sizes in ACZ catalysts slightly increased with the reduction temperature because of SSA degradation. However, OSC-c increased with the reduction temperature, despite the growth of Pt particles. These results also suggest that OSC-c is affected by the behavior of oxygen, rather than Pt particle size, as discussed in Section 3.1.

On the other hand, OSC-r of ACZ catalysts shown in Fig. 11 indicates the different variation from OSC-c of corresponding catalysts against the evaluation temperature and the reduction temperature. Namely, the OSC-r measured below 200 °C showed a maximum value against the reduction temperature at 800 °C, whereas that at 300 °C increased with the reduction temperature.

As in the previous publications [21], the reductive treatment improved the structural homogeneity of Ce and Zr ions arrangement in the $CeZrO_4$ crystal lattice, but decreased the SSA of an oxide. The Ce and Zr ions arrangement in the $CeZrO_4$ crystal lattice turns more regular with the reductive temperature. The structural homogeneity in the $CeZrO_4$ crystal lattice facilitates the oxygen diffusion, in other words, highly mobile oxygen is apt to be produced in the lattice, such as the κ-phase with regularly arranged Ce and Zr ions. Higher reduction temperature favors the formation of regular Ce and Zr ions arrangement, but decreases the SSA of catalysts, leading to the drop of releasable oxygen amount on or near surface and to variation of

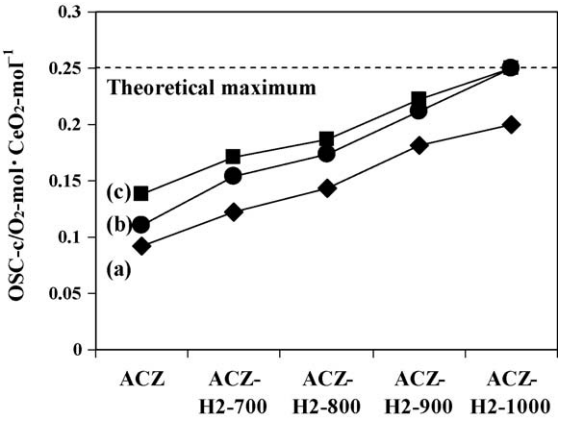

Fig. 10. OSC-c of ACZ catalysts reduced in H_2 (5%)/N_2 for 5 h prior to Pt loading. ACZ: fresh (not reduced); ACZ-H2-700: reduced at 700 °C; ACZ-H2-800: reduced at 800 °C; ACZ-H2-900: reduced at 900 °C; ACZ-H2-1000: reduced at 1000 °C. (a) Measured at 100 °C, (b) measured at 300 °C, and (c) measured at 500 °C. The dotted-line shows the theoretical maximum, which corresponds to the state of that $Ce_2Zr_2O_7$ in a reductive atmosphere and $Ce_2Zr_2O_8$ in an oxidation condition.

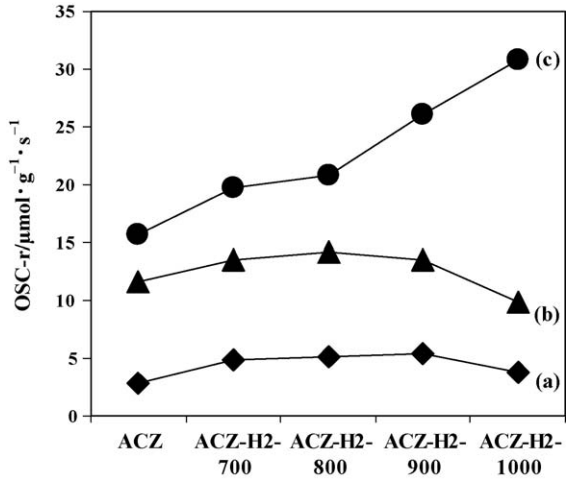

Fig. 11. OSC-r of ACZ catalysts reduced in H_2 (5%)/N_2 for 5 h prior to Pt loading. The measurement was performed using a fixed-bed flow-type reactor with alternative CO/N_2 and O_2/N_2 at (a) 100 °C, (b) 200 °C, and (c) 300 °C. ACZ: fresh (not reduced); ACZ-H2-700: reduced at 700 °C; ACZ-H2-800: reduced at 800 °C; ACZ-H2-900: reduced at 900 °C; ACZ-H2-1000: reduced at 1000 °C.

Pt–O–Ce interaction. Hence, the order of OSC-r should be considered from these two perspectives.

As shown in Fig. 12, below 800 °C reductive pretreatments, the top of the main peak of ACZ at around 140 °C shifted to lower temperature, and in contrast, above 900 °C reductive pretreatments, it shifted to higher. Each main peak for these catalysts is identified as the reduction of Pt oxide and $CeZrO_4$ by Pt as discussed in Section 3.1. Therefore, the peak shift to lower temperature implies that reductive pretreatments below 800 °C make the hydrogen spill over for reduction of $CeZrO_4$ easier due to the weaker Pt–O–Ce interaction. On the other hand, the peak shift to higher temperature above 900 °C reductive pretreatments is corresponding to the difficulty of the hydrogen spill over. As discussed earlier, it seems that the variation of Pt–O–Ce interaction may have some relation with the Ce ions concentration on the $CeZrO_4$ crystallite surface and SSA after the reductive pretreatment; however, further investigation is needed to confirm the phenomena near future.

Furthermore, these catalysts showed almost identical Pt particle sizes, except ACZ-H2-1000, as shown in Table 2, and the order of reductive peak temperature for these catalysts is

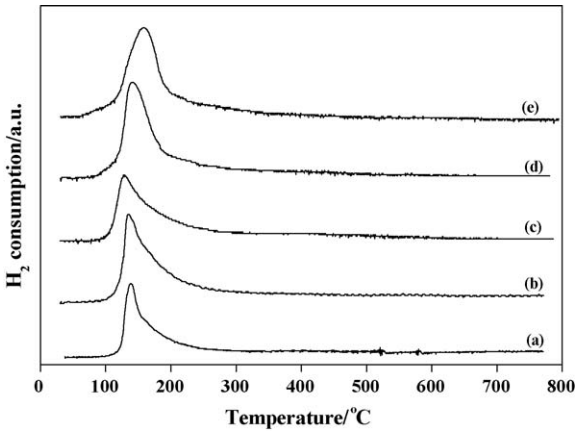

Fig. 12. H_2-TPR profiles of catalysts reduced in H_2 (5%)/N_2 at (b) 700 °C, (c) 800 °C, (d) 900 °C, and (e) 1000 °C for 5 h; (a) was fresh (not treated) catalyst. All catalysts were preheated prior to Pt loading.

comparatively similar with that of OSC-r below 200 °C. Theses results imply that OSC-r is predominated simultaneously by the reduction of Pt oxide and the oxygen releasing from $CeZrO_4$ reduced by the reduced Pt metal. Therefore, OSC-r evaluated below 200 °C shows a maximum value against the pre-reduction temperature at 800 °C and it is consistent with the result of H_2-TPR. In addition, the OSC-r of ACZ did not increase apparently from 200 to 300 °C. This result suggests that oxygen on or near the surface in ACZ is released mainly.

Along with increasing the evaluation temperature for OSC-r to 300 °C, the change of Pt from oxide to metal is promoted sufficiently and the oxygen diffusion in the $CeZrO_4$ crystal lattice is also enhanced in the κ-phase which has the orderly arranged Ce and Zr cation structure, especially for the ACZ-H2-1000. Thus, the OSC-r also increased with the reduction temperature as well as the OSC-c.

The above results indicate that OSC-r is determined by the following two factors: (i) the generation of highly mobile oxygen in the $CeZrO_4$ lattice, (ii) the reductive property of Pt oxide and that of $CeZrO_4$ by the reduced Pt, which could be attributed to the SSA. The pretreatment conditions such as the reduction temperature should be determined according to the practical conditions of a three-way catalyst.

4. Conclusion

To enhance OSC properties, ACZ was treated under various atmospheres. Reductive treatments at temperatures from 700 to 1000 °C achieved large improvement in the complete oxygen storage capacity (OSC-c). ACZ reduction of 1000 °C prior to Pt loading (ACZ-H2-1000), in particular, indicated the theoretical maximum OSC-c, while maintaining a sufficient SSA. This high-performance OSC-c could be derived from the formation of the κ-phase of the $CeZrO_4$ crystallite, where Ce and Zr ions arrange regularly.

The reductive treatment also improved the oxygen release rate (OSC-r) of the ACZ catalyst; however, its variation against the evaluation temperature and the reduction temperature differed from that of OSC-c. The OSC-r of ACZ catalysts measured below 200 °C showed a maximum value against the reduction temperature at 800 °C, whereas that at 300 °C increased with the reduction temperature, as in the case of OSC-c.

Introducing Al_2O_3 facilitates maintaining of a reasonable SSA of ACZ as well as the formation of the κ-phase of $CeZrO_4$ crystallite after reductive treatments. This provides the appropriately designed OSC material as well as a guiding principle for the development of OSC material with a much higher performance in near future.

Acknowledgments

The authors would like to thank the members of the Catalyst Laboratory, Toyota Central R&D Labs., Inc.

References

[1] H.S. Gandhi, A.G. Piken, M. Shelef, R.G. Delesh, SAE Paper No. 760201, 1976.
[2] H.C. Yao, Y.F. Yu Yao, J. Catal. 86 (1984) 254.
[3] T. Kanazawa, J. Suzuki, T. Takada, T. Suzuki, A. Morikawa, A. Suda, H. Sobukawa, M. Sugiura, SAE Paper No. 2003-01-0811, 2003.
[4] H. He, H.X. Dai, L.H. Ng, K.W. Wong, C.T. Au, J. Catal. 206 (2002) 1.
[5] D. Terribile, A. Trovarelli, J. Llorca, C. de Leitenburg, G. Dolcetti, Catal. Today 43 (1998) 79.
[6] S. Matsumoto, N. Miyoshi, T. Kanazawa, M. Kimura, M. Ozawa, S. Yoshida, N. Tabezawa, T. Ono, Catalysis Science and Technology, vol. 1, Kodansha/VCH, Tokyo/Weinheim, 1991, p. 335.
[7] M. Ozawa, M. Kimura, A. Isogai, J. Alloys Compd. 193 (1993) 73.
[8] A. Suda, T. Kandori, Y. Ukyo, H. Sobukawa, M. Sugiura, J. Ceram. Soc. Jpn. 108 (2000) 473.

[9] A. Suda, H. Sobukawa, T. Suzuki, T. Kandori, Y. Ukyo, M. Sugiura, J. Ceram. Soc. Jpn. 109 (2001) 177.
[10] A. Suda, H. Sobukawa, T. Suzuki, T. Kandori, Y. Ukyo, M. Sugiura, J. Ceram. Soc. Jpn. 110 (2002) 126.
[11] A. Morikawa, T. Suzuki, T. Kanazawa, K. Kikuta, A. Suda, H. Shinjo, Appl. Catal. B 78 (2008) 210.
[12] S. Matsumoto, Catal. Today 90 (2004) 183.
[13] Y. Nagai, T. Yamamoto, T. Tanaka, S. Yoshida, T. Nonaka, T. Okamoto, A. Suda, M. Sugiura, Catal. Today 74 (2002) 225.
[14] F. Fally, V. Perrichon, H. Vidal, J. Kašpar, G. Blanco, J.M. Pintado, S. Bernal, G. Colon, M. Daturi, J.C. Lavalley, Catal. Today 59 (2000) 373.
[15] H. Vidal, S. Bernal, J. Kašpar, M. Pijolat, V. Perrichon, G. Blanco, J.M. Pintado, R.T. Baker, G. Colon, F. Fally, Catal. Today 54 (1999) 93.
[16] H. Vidal, J. Kašpar, M. Pijolat, G. Colon, S. Bernal, A. Cordón, V. Perrichon, F. Fally, Appl. Catal. B 27 (2000) 49.
[17] H. Vidal, J. Kašpar, M. Pijolat, G. Colon, S. Bernal, A. Cordón, V. Perrichon, F. Fally, Appl. Catal. B 30 (2001) 75.
[18] S.J. Wilson, G.D. McConneil, J. Solid State Chem. 34 (1980) 315.
[19] Reference Catalyst Committee, Catalysis Society of Japan, Catal. Catal. 28 (1986) 41.
[20] Reference Catalyst Committee, Catalysis Society of Japan, Catal. Catal. 31 (1989) 317.
[21] T. Tanabe, A. Suda, C. Desorme, D. Duprez, H. Shinjyoh, M. Sugiura, Stud. Sci. Catal. 138 (2001) 135.
[22] H. Kishimoto, T. Omata, S. Otsuka-Yao-Matsuo, K. Ueda, H. Hosono, H. Kawazoe, J. Alloy. Compd. 312 (2000) 94.
[23] M. Yashima, S. Sasaki, Y. Yamaguchi, M. Kakihana, M. Yoshimura, T. Mori, Appl. Phys. Lett. 72 (1998) 182.
[24] N. Izu, H. Kishimoto, T. Omata, T. Yao, S. Otsuka-Yao-Matsuo, Sci. Technol. Adv. Mater. 2 (2001) 443.
[25] T. Yamamoto, A. Suzuki, Y. Nagai, T. Tanabe, F. Dong, Y. Inada, M. Nomura, M. Tada, Y. Iwasawa, Angew. Chem. Int. Ed. 46 (2007) 9253.
[26] Z. Chen, N. Ho, P. Shen, Mater. Sci. Eng. A 196 (1995) 253.
[27] S. Damyanova, C.A. Perez, M. Schmal, J.M.C. Bueno, Appl. Catal. A 234 (2002) 271.
[28] T. Masui, Y. Peng, K. Machida, G. Adachi, Chem. Mater. 10 (1998) 4005.
[29] T. Ozaki, T. Masui, K. Machida, G. Adachi, T. Sakata, H. Mori, Chem. Mater. 12 (2000) 643.
[30] A. Suda, K. Yamamura, H. Sobukawa, Y. Ukyo, T. Tanabe, Y. Nagai, F. Dong, M. Sugiura, J. Ceram. Soc. Jpn. 112 (2004) 623.
[31] H. Shinjo, H. Muraki, Y. Fujitani, Appl. Catal. 49 (1989) 195.
[32] F. Dong, A. Suda, T. Tanabe, Y. Nagai, H. Sobukaw, H. Shinjo, M. Sugiura, C. Descorme, D. Duprez, Catal. Today 93–95 (2004) 827.
[33] S. Damyanova, J.M.C. Bueno, Appl. Catal. A 253 (2003) 135.
[34] J. Kaspar, P. Fornasiero, M. Graziani, Catal. Today 50 (1999) 285.
[35] F.B. Passos, E.R. de Oliveira, L.V. Mattos, F.B. Noronha, Catal. Today 101 (2005) 23.
[36] P. Fornasiero, J. Kaspar, T. Montini, M. Graziani, V. Dal Santo, R. Psaro, S. Recchia, J. Mol. Catal. A 204–205 (2003) 683.
[37] R. Pérez-Hernández, F. Aguilar, A. Gómez-Cortés, G. Díaz, Catal. Today 107–108 (2005) 175.
[38] Y. Nagai, T. Hirabayashi, K. Dohmae, N. Takagi, T. Minami, Hi. Shinjoh, S. Matsumoto, J. Catal. 242 (2006) 103.
[39] C.P. Hwang, C.T. Yeh, J. Mol. Catal. A: Chem. 112 (1996) 295.
[40] T. Sasaki, Y. Ukyo, A. Suda, M. Sugiura, K. Kuroda, S. Arai, H. Saka, J. Ceram. Soc. Jpn. 111 (2003) 382.
[41] J. Fan, X. Wu, R. Ran, D. Weng, Appl. Surf. Sci. 245 (2005) 162.
[42] T. Sasaki, Y. Ukyo, K. Kuroda, S. Arai, S. Muto, H. Saka, J. Ceram. Soc. Jpn. 112 (2004) 440.